ChemComm

COMMUNICATION

View Article Online
View Journal | View Issue

Open Access Article. Published on 05 September 2014. Downloaded on 8/12/2024 4:00:51 AM.
This article is licensed under a Creative Commons Attribution 3.0 Unported Licence.

Cite this: *Chem. Commun.*, 2014, **50**, 12772

Received 15th July 2014,
Accepted 4th September 2014

DOI: 10.1039/c4cc05438e

www.rsc.org/chemcomm

Highly unusual interpenetration isomers of electroactive nickel bis(dithiolene) coordination frameworks†

Thomas B. Faust, Pavel M. Usov, Deanna M. D'Alessandro* and Cameron J. Kepert*

The metalloligand $[Ni(pedt)_2]^-$ (pedt = 1-(pyridine-4-yl)ethylene-1,2-dithiolate) has been incorporated into two multi-dimensional structures for the first time. These coordination frameworks represent highly unusual interpenetration isomers and exhibit solid state redox and optical properties that reflect the electronically delocalised nature of the metalloligand.

Metallodithiolenes represent an intriguing class of compounds due to their capacity to undergo organic-centred redox processes and the creation of stable radical states. As such, they have been subject to intense investigation for their electroactive, conductive and magnetic properties.[1–3] Despite the considerable potential of $[Ni(pedt)_2]^{n-}$ (n = 0, 1, 2) as a non-innocent component in multidimensional materials, coordination to a secondary metal centre *via* pyridyl binding has been reported just once to date, and then only in a discrete assembly where the metalloligand was charge neutral and diamagnetic.[4] It has also been synthesised as a discrete neutral species,[5] monoanion,[6,7] dianion,[6] and diprotonated monocation.[7] The pendant 4-pyridyl groups are well suited for metal ligation and in the radical monoanionic state this may be expected to be particularly favourable both for electrostatic and charge-balance reasons, the latter removing the necessity for a counterion. Its planar conformation is reminiscent of simpler, oft-used pillars in metal–organic frameworks and more generally in coordination polymers. Allied to this, the potential for rich redox chemistry, the presence of paramagnetism in the native monoanionic state and an extensive π-system renders $[Ni(pedt)_2]^{n-}$ an ideal ligand for the creation of materials with interesting electronic and magnetic properties. The ability to manipulate the electronic structure promises possible implementation as a redox-active switch in promoting or attenuating long-range exchange processes.

The reaction of $[Ni(pedt)_2][Et_4N]$ with $Zn(NO_3)_2{\cdot}xH_2O$ in DMF at room temperature yielded two crystalline phases, **1** and **2**, which are interpenetration isomers of one another.‡ Such isomers arise when frameworks possess nets with identical topologies but differing degrees of interpenetration. The observation of such a phenomenon is relatively scarce since subtle alteration in reaction conditions rarely forms multiple distinct frameworks, whilst larger changes often encourage the formation of different, non-isomeric frameworks.[8,9]

1 consists of non-interpenetrated stacks of (4,4) sheets whilst **2** possesses 2D inclined two-fold interpenetration of three sets of (4,4) sheets. The nets have the same molecular formula (excluding solvent), $\{M[Ni(pedt)_2]_2(solvent)_2\}$, and connectivity (see Fig. 1 and 2), differing only slightly in their geometry; **1** possesses a kite-shaped grid, while **2** is nearer to square-shaped (see ESI,† Fig. S4). A phase-pure sample of **1** can be synthesised by performing the reaction in mixed solvents (DMF–EtOH), which expedites crystallisation. The onset of crystallisation is instantaneous and the product can be harvested in reasonable yield immediately or in higher yield after 24 h. By contrast, crystallisation of **2** in DMF only becomes

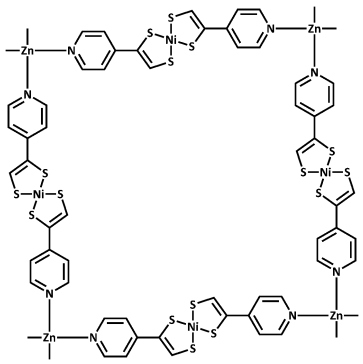

Fig. 1 Connectivity of the 2D grid in **1** and **2**; solvent bound to the axial positions on Zn not shown.

School of Chemistry, University of Sydney, NSW 2006, Australia.
E-mail: deanna.dalessandro@sydney.edu.au, cameron.kepert@sydney.edu.au

† Electronic supplementary information (ESI) available: Including details for ligand synthesis, powder X-ray diffraction, single crystal X-ray diffraction, electrochemistry, UV/Vis/NIR spectroscopy, IR spectroscopy, and thermogravimetric analysis. CCDC 1011922 (**1**) and 1011920 (**2**). For ESI and crystallographic data in CIF or other electronic format see DOI: 10.1039/c4cc05438e

This journal is © The Royal Society of Chemistry 2014

Open Access Article. Published on 05 September 2014. Downloaded on 8/12/2024 4:00:51 AM.
This article is licensed under a Creative Commons Attribution 3.0 Unported Licence.

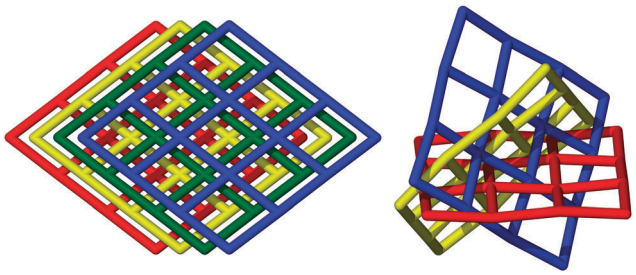

Fig. 2 Cartoon representation of **1** (left) and **2** (right), each colour represents a discrete 2D net.

apparent after a few days, and is concomitant with the growth of **1** (see ESI,† Fig. S3). Leaving the solution for extended periods of time does not appear to increase the ratio of phase **2** over **1**, and separation of the phases was only possible by manual manipulation, yielding insufficient quantities for analyses beyond single crystal X-ray diffraction measurement for **2**.

1 crystallises in the monoclinic space group $C2/c$ and **2** in the trigonal space group $C3_1/c$. The connectivities of **1** and **2** are identical; each octahedral zinc ion is bound axially by solvent molecules and equatorially by the pyridyl nitrogen of $[Ni(pedt)_2]^-$. The metalloligands consist of two pedt moieties, each bound in a bidentate fashion (κ^2S,S') to a central square planar nickel. The pyridyl groups are distal, *i.e.*, the metalloligand is in a *trans* configuration. All four metalloligands extend within the plane to ligate to another Zn centre. In this way, a two dimensional (4,4) network is formed. In **1** the 2D layers are planar and are described by the Miller index $(20\bar{4})$ separated by a distance of 3.779 Å, with the layers stacking only in the c direction.

For **2**, the layers corrugate slightly about a mean plane with ridges running along c (see ESI,† Fig. S5). The layers are now described by the Miller indices (020), (200) and $(2\bar{2}0)$. The overall topology of **2** consists of three stacks of 2D sheets with a common axis down c, at angles of 60° to one another. Every window is penetrated by just one other net (two-fold interpenetrated). The distance between each layer within a stack is now dictated by the periodicity of the windows ($\sqrt{3}/2a$ = 21.9 Å), rather than the van der Waals forces between the layers as in **1**. So whilst **1** contains only moderate voids in the grid windows (20% solvent accessible with unbound solvent artificially removed), **2** possesses large triangular channels with edges in excess of 20 Å. These channels are connected through pores along a and b resulting in 75% solvent accessible void (calculated with 0.1 Å grid spacing and 1.2 Å probe radius) (see Fig. 3). Rather unusually, this observation is contrary to the general consensus which suggests that interpenetration suppresses porosity.

It is unusual for the less densely packed phase to be the thermodynamic product. Stabilisation of this much more open phase appears to be associated with the more favourable interlayer interactions achieved through interpenetration at the expense of the entropic penalty commonly associated with the formation of more open framework systems (see ESI,† Section 4 for a more thorough discussion). The structure of **2** is unusual even in isolation since examples in which more than two stacks of 2D sheets are present appear very limited.[10–13]

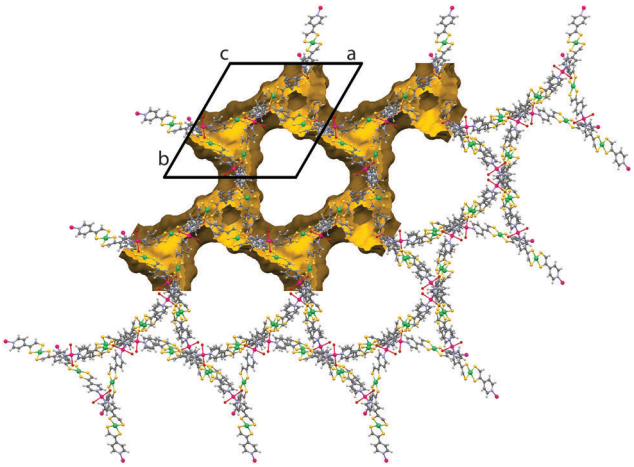

Fig. 3 Crystal structure of **2** exhibiting very large triangular pores, viewed down the c axis. The unit cell is indicated in black and the solvent accessible surface indicated in yellow.

The electronic properties of the $[Ni(pedt)_2]^{n-}$ metalloligand have recently been investigated in some detail by Zhu and Dai, who concluded that its associated redox chemistry is neither wholly metal nor organic based, preferring to call the nickel bis(dithiolate) unit, $[Ni(edt)_2]$, an 'indivisible moiety'.[7] Thus, rather than assign formal charges and oxidation states one shall only consider the accessible states as $[Ni(edt)_2]^{0/-1/-2}$. For materials such as **1** to be of electronic and magnetic interest, it is vital that these fundamental properties be retained in the framework, and we therefore undertook spectroscopic and electrochemical studies to confirm their retention.

Solid state UV-Vis-NIR of the metalloligand $[Ni(pedt)_2][Et_4N]$ replicated that previously reported in solution;[7] namely an intense low energy absorption in the NIR, relatively weak intramolecular charge transfer (ICT) absorptions circa 20 000 cm^{-1} (500 nm) (which are poorly resolved in the solid state), and additional ICT bands above 25 000 cm^{-1} (400 nm) (see Fig. 4).

Measurement of **1** revealed that the NIR transition shifted only 7 nm (80 cm^{-1}) to lower energy upon incorporation of the ligand into the framework, whilst the high energy ICT bands above 25 000 cm^{-1} remain predominantly the same. The decrease in intensity of the peak at 20 000 cm^{-1} and corresponding appearance of a peak at 16 400 cm^{-1} (610 nm) results from the coordination of the pyridyls to the Zn(II), which increases their electron accepting

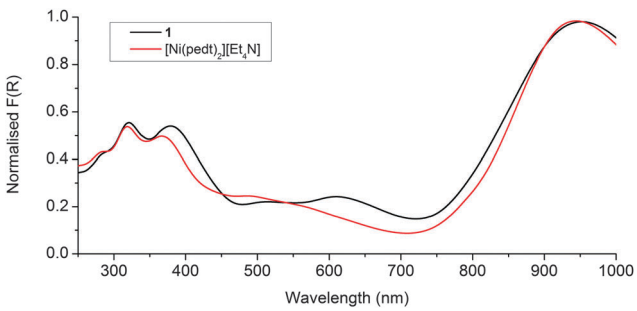

Fig. 4 Solid state UV-Vis-NIR of **1** (black) and $[Ni(pedt)_2][Et_4N]$ (red).

Open Access Article. Published on 05 September 2014. Downloaded on 8/12/2024 4:00:51 AM.
This article is licensed under a Creative Commons Attribution 3.0 Unported Licence.

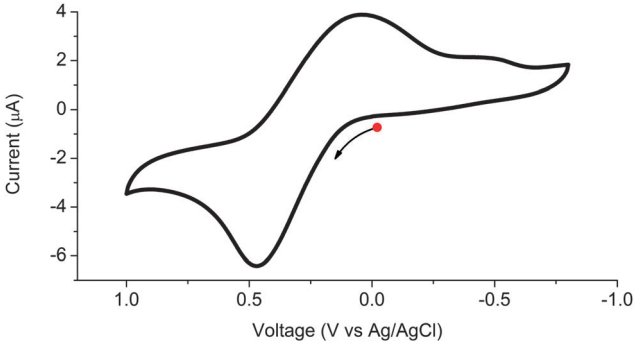

Fig. 5 Solid state cyclic voltammogram of **1** in aqueous 0.1 M KCl electrolyte, where the arrow indicates the direction of the forward scan.

nature and thus narrows the SOMO → LUMO gap (see Fig. 4). Such an observation has previously been reported for $[Ni(Hpedt)_2]^+$.[7] These data suggest that the radical/paramagnetic nature of the metalloligand is indeed maintained in the framework.

$[Ni(pedt_2)][Et_4N]$ is known to possess three accessible redox states;[7] the monoanionic dithiolate core undergoes one reversible oxidation process to the neutral species and a reversible reduction to the dianion (see ESI,† Fig. S7).

The redox behaviour of **1** was investigated using solid state cyclic voltammetry in aqueous 0.1 M KCl electrolyte (see Fig. 5). The framework was found to undergo a single reversible oxidation process at $E_{1/2}$ = 0.26 V (*vs.* Ag/AgCl) corresponding to oxidation of the ligand. The redox couple is largely reversible as indicated by its I_a/I_c value of 0.72; however, ΔE = 420 mV is significantly larger than the 57 mV expected for a one electron process.[14] This behaviour has been observed previously in solid state electrochemistry and has been attributed to the energy barrier for solid–solid transformation.[15] A second peak assigned to reduction of the ligand was observed at −0.51 V. The irreversible nature of this second process suggests that the framework is unstable to formation of the dianion. We may therefore deduce that the metalloligand can be cycled between its paramagnetic monoanionic state and diamagnetic neutral state upon exposure of the framework to a suitable potential, applied either by chemical or electrochemical means.

In summary, the metalloligand $[Ni(pedt)_2]^-$ has been incorporated into a coordination framework where it retains its redox activity for the oxidation couple, which may have special consequence in high magnitude spin environments.[16] Work is underway to investigate the potential for incorporation of magnetically interesting divalent metals into similar systems and to probe the possibility of switchable electronic and magnetic exchange mediated by the redox active ligand. We also present a second framework which is an interpenetration isomer of the first, yet presents a starkly different 3D topology that to our knowledge is unique.

Financial support for this work was provided by the Australian Research Council. Collection of single crystal diffraction data of **2** was undertaken on the MX2 beamline at the Australian Synchrotron, Victoria, Australia, and we thank them for access to their facilities.

Notes and references

‡ Synthesis of non-interpenetrated $\{Zn[Ni(pedt)_2]_2(DMF)_2\}\cdot 2(DMF)$, ($C_{40}H_{48}N_8Ni_2O_4S_8Zn$, **1**): in a 20 mL glass vial $[Ni(pedt)_2][Et_4N]$ (53 mg, 0.10 mmol) was dissolved in DMF/EtOH (5 mL, 1 : 1). $Zn(NO_3)_2\cdot xH_2O$ (15 mg, 0.05 mmol) dissolved in DMF/EtOH (5 mL, 1 : 1) was added expeditiously, a plastic lid attached and the reaction vessel shaken vigorously. The reaction was left to proceed for 24 h after which the solution was filtered and washed with DMF (100 mL) and DMF/EtOH (100 mL, 1 : 1), to yield a dark purple microcrystalline product (70%, 40 mg, 0.035 mmol). Synthesis of interpenetrated $\{Zn[Ni(pedt)_2]_2(solvent)_2\}\cdot x(solvent)$, ($C_{28}H_{20}N_4Ni_2O_2S_8Zn$, **2**): in a 20 mL glass vial $[Ni(pedt)_2][Et_4N]$ (53 mg, 0.10 mmol) was dissolved in DMF (5 mL). $Zn(NO_3)_2\cdot xH_2O$ (15 mg, 0.05 mmol) dissolved in DMF (5 mL) was added expeditiously, a plastic lid attached and the reaction vessel shaken vigorously. The reaction was left to proceed for one week before large dark purple single crystals of **2** were removed. Single crystals of **2** are easily distinguished from **1** as they possess one long axis.

1 R. Eisenberg and H. B. Gray, *Inorg. Chem.*, 2011, **50**, 9741–9751.
2 R. Kato, *Chem. Rev.*, 2004, **104**, 5319–5346.
3 N. Robertson and L. Cronin, *Coord. Chem. Rev.*, 2002, **227**, 93–127.
4 R. Wang, L.-C. Kang, J. Xiong, X.-W. Dou, X.-Y. Chen, J.-L. Zuo and X.-Z. You, *Dalton Trans.*, 2011, **40**, 919–926.
5 S. Rabaça, A. C. Cerdeira, S. Oliveira, I. C. Santos, R. T. Henriques, L. C. J. Pereira, J. T. Coutinho and M. Almeida, *Polyhedron*, 2012, **39**, 91–98.
6 S. Rabaça, D. Belo, A. C. Cerdeira, S. I. G. Dias, M. B. C. Branco, L. C. J. Pereira, I. C. Santos, M. Fourmigue and M. Almeida, *CrystEngComm*, 2009, **11**, 2154–2159.
7 X.-Y. Li, Y.-G. Sun, P. Huo, M.-Y. Shao, S.-F. Ji, Q.-Y. Zhu and J. Dai, *Phys. Chem. Chem. Phys.*, 2013, **15**, 4016–4023.
8 T. A. Makal, A. A. Yakovenko and H.-C. Zhou, *J. Phys. Chem. Lett.*, 2011, **2**, 1682–1689.
9 H.-L. Jiang, T. A. Makal and H.-C. Zhou, *Coord. Chem. Rev.*, 2013, **257**, 2232–2249.
10 C. B. Aakeröy, A. M. Beatty and D. S. Leinen, *Angew. Chem., Int. Ed.*, 1999, **38**, 1815–1819.
11 N. Moliner, C. Muñoz, S. Letard, X. Solans, N. Menendez, A. Goujon, F. Varret and J. A. Real, *Inorg. Chem.*, 2000, **39**, 5390–5393.
12 L. Carlucci, G. Ciani, D. M. Proserpio and S. Rizzato, *CrystEngComm*, 2003, **5**, 190–199.
13 M. Kondo, M. Shimamura, S.-i. Noro, S. Minakoshi, A. Asami, K. Seki and S. Kitagawa, *Chem. Mater.*, 2000, **12**, 1288–1299.
14 A. Bard and L. Faulkner, *Electrochemical Methods: Fundamentals and Applications*, John Wiley & Sons, Inc, 2001.
15 A. M. Bond, S. Fletcher, F. Marken, S. J. Shaw and P. G. Symons, *J. Chem. Soc., Faraday Trans.*, 1996, **92**, 3925–3933.
16 T. B. Faust and D. M. D'Alessandro, *RSC Adv.*, 2014, **4**, 17498–17512.

 This journal is © The Royal Society of Chemistry 2014